arXiv:1011.0885v1 [hep-ex] 3 Nov 2010

Evidence for ψ' decays into $\gamma\pi^0$ and $\gamma\eta$

M. Ablikim[1], M. N. Achasov[5], L. An[9], Q. An[35], Z. H. An[1], J. Z. Bai[1], R. Baldini[17], Y. Ban[22], J. Becker[2], N. Berger[1], M. Bertani[17], J. M. Bian[1], I. Boyko[15], R. A. Briere[3], V. Bytev[15], X. Cai[1], G. F. Cao[1], X. X. Cao[1], J. F. Chang[1], G. Chelkov[15a], G. Chen[1], H. S. Chen[1], J. C. Chen[1], M. L. Chen[1], S. J. Chen[20], Y. Chen[1], Y. B. Chen[1], H. P. Cheng[11], Y. P. Chu[1], D. Cronin-Hennessy[34], H. L. Dai[1], J. P. Dai[1], D. Dedovich[15], Z. Y. Deng[1], I. Denysenko[15b], M. Destefanis[37], Y. Ding[18], L. Y. Dong[1], M. Y. Dong[1], S. X. Du[41], M. Y. Duan[25], R. R. Fan[1], J. Fang[1], S. S. Fang[1], F. Feldbauer[2], C. Q. Feng[35], C. D. Fu[1], J. L. Fu[20], Y. Gao[31], C. Geng[35], K. Goetzen[7], W. X. Gong[1], M. Greco[37], S. Grishin[15], M. H. Gu[1], Y. T. Gu[9], Y. H. Guan[6], A. Q. Guo[21], L. B. Guo[19], Y.P. Guo[21], X. Q. Hao[1], F. A. Harris[33], K. L. He[1], M. He[1], Z. Y. He[21], Y. K. Heng[1], Z. L. Hou[1], H. M. Hu[1], J. F. Hu[6], T. Hu[1], B. Huang[1], G. M. Huang[12], J. S. Huang[10], X. T. Huang[24], Y. P. Huang[1], T. Hussain[36], C. S. Ji[35], Q. Ji[1], X. B. Ji[1], X. L. Ji[1], L. K. Jia[1], L. L. Jiang[1], X. S. Jiang[1], J. B. Jiao[24], Z. Jiao[11], D. P. Jin[1], S. Jin[1], F. F. Jing[31], M. Kavatsyuk[16], S. Komamiya[30], W. Kuehn[32], J. S. Lange[32], J. K. C. Leung[29], Cheng Li[35], Cui Li[35], D. M. Li[41], F. Li[1], G. Li[1], H. B. Li[1], J. C. Li[1], Lei Li[1], N. B. Li[19], Q. J. Li[1], W. D. Li[1], W. G. Li[1], X. L. Li[24], X. N. Li[1], X. Q. Li[21], X. R. Li[1], Z. B. Li[27], H. Liang[35], Y. F. Liang[26], Y. T. Liang[32], G. R Liao[8], X. T. Liao[1], B. J. Liu[28], B. J. Liu[29], C. L. Liu[3], C. X. Liu[1], C. Y. Liu[1], F. H. Liu[25], Fang Liu[1], Feng Liu[12], G. C. Liu[1], H. Liu[1], H. B. Liu[6], H. M. Liu[1], H. W. Liu[1], J. P. Liu[39], K. Liu[22], K. Y Liu[18], Q. Liu[33], S. B. Liu[35], X. H. Liu[1], Y. B. Liu[21], Y. W. Liu[35], Yong Liu[1], Z. A. Liu[1], Z. Q. Liu[1], H. Loehner[16], G. R. Lu[10], H. J. Lu[11], J. G. Lu[1], Q. W. Lu[25], X. R. Lu[6], Y. P. Lu[1], C. L. Luo[19], M. X. Luo[40], T. Luo[1], X. L. Luo[1], C. L. Ma[6], F. C. Ma[18], H. L. Ma[1], Q. M. Ma[1], T. Ma[1], X. Ma[1], X. Y. Ma[1], M. Maggiora[37], Q. A. Malik[36], H. Mao[1], Y. J. Mao[22], Z. P. Mao[1], J. G. Messchendorp[16], J. Min[1], R. E. Mitchell[14], X. H. Mo[1], C. Motzko[2], N. Yu. Muchnoi[5], Y. Nefedov[15], Z. Ning[1], S. L. Olsen[23], Q. Ouyang[1], S. Pacetti[17], M. Pelizaeus[33], K. Peters[7], J. L. Ping[19], R. G. Ping[1], R. Poling[34], C. S. J. Pun[29], M. Qi[20], S. Qian[1], C. F. Qiao[6], X. S. Qin[1], J. F. Qiu[1], K. H. Rashid[36], G. Rong[1], X. D. Ruan[9], A. Sarantsev[15c], J. Schulze[2], M. Shao[35], C. P. Shen[33], X. Y. Shen[1], H. Y. Sheng[1], M. R. Shepherd[14], X. Y. Song[1], S. Sonoda[30], S. Spataro[37], B. Spruck[32], D. H. Sun[1], G. X. Sun[1], J. F. Sun[10], S. S. Sun[1], X. D. Sun[1], Y. J. Sun[35], Y. Z. Sun[1], Z. J. Sun[1], Z. T. Sun[35], C. J. Tang[26], X. Tang[1], X. F. Tang[8], H. L. Tian[1], D. Toth[34], G. S. Varner[33], X. Wan[1], B. Q. Wang[22], K. Wang[1], L. L. Wang[4], L. S. Wang[1], P. Wang[1], P. L. Wang[1], Q. Wang[1], S. G. Wang[22], X. L. Wang[35], Y. D. Wang[35], Y. F. Wang[1], Y. Q. Wang[24], Z. Wang[1], Z. G. Wang[1], Z. Y. Wang[1], D. H. Wei[8], S. P. Wen[1], U. Wiedner[2], L. H. Wu[1], N. Wu[1], W. Wu[18], Z. Wu[1], Z. J. Xiao[19], Y. G. Xie[1], G. F. Xu[1], G. M. Xu[22], H. Xu[1], Y. Xu[21], Z. R. Xu[35], Z. Z. Xu[35], Z. Xue[1], L. Yan[35], W. B. Yan[35], Y. H. Yan[13], H. X. Yang[1], M. Yang[1], T. Yang[9], Y. Yang[12], Y. X. Yang[8], M. Ye[1], M.H. Ye[4], B. X. Yu[1], C. X. Yu[21], L. Yu[12], C. Z. Yuan[1], W. L. Yuan[19], Y. Yuan[1], A. A. Zafar[36], A. Zallo[17], Y. Zeng[13], B. X. Zhang[1], B. Y. Zhang[1], C. C. Zhang[1], D. H. Zhang[1], H. H. Zhang[27], H. Y. Zhang[1], J. Zhang[19], J. W. Zhang[1], J. Y. Zhang[1], J. Z. Zhang[1], L. Zhang[20], S. H. Zhang[1], T. R. Zhang[19], X. J. Zhang[1], X. Y. Zhang[24], Y. Zhang[1], Y. H. Zhang[1], Z. P. Zhang[35], Z. Y. Zhang[39], G. Zhao[1], H. S. Zhao[1], Jiawei Zhao[35], Jingwei Zhao[1], Lei Zhao[35], Ling Zhao[1], M. G. Zhao[21], Q. Zhao[1], S. J. Zhao[41], T. C. Zhao[38], X. H. Zhao[20], Y. B. Zhao[1], Z. G. Zhao[35], Z. L. Zhao[9], A. Zhemchugov[15a], B. Zheng[1], J. P. Zheng[1], Y. H. Zheng[6], Z. P. Zheng[1], B. Zhong[1], J. Zhong[2], L. Zhong[31], L. Zhou[1], X. K. Zhou[6], X. R. Zhou[35], C. Zhu[1], K. Zhu[1], K. J. Zhu[1], S. H. Zhu[1], X. L. Zhu[31], X. W. Zhu[1], Y. S. Zhu[1], Z. A. Zhu[1], J. Zhuang[1], B. S. Zou[1], J. H. Zou[1], J. X. Zuo[1], P. Zweber[34]

(BESIII Collaboration)

[1] *Institute of High Energy Physics, Beijing 100049, P. R. China*
[2] *Bochum Ruhr-University, 44780 Bochum, Germany*
[3] *Carnegie Mellon University, Pittsburgh, PA 15213, USA*
[4] *China Center of Advanced Science and Technology, Beijing 100190, P. R. China*
[5] *G.I. Budker Institute of Nuclear Physics SB RAS (BINP), Novosibirsk 630090, Russia*
[6] *Graduate University of Chinese Academy of Sciences, Beijing 100049, P. R. China*
[7] *GSI Helmholtzcentre for Heavy Ion Research GmbH, D-64291 Darmstadt, Germany*
[8] *Guangxi Normal University, Guilin 541004, P. R. China*
[9] *Guangxi University, Naning 530004, P. R. China*
[10] *Henan Normal University, Xinxiang 453007, P. R. China*
[11] *Huangshan College, Huangshan 245000, P. R. China*
[12] *Huazhong Normal University, Wuhan 430079, P. R. China*
[13] *Hunan University, Changsha 410082, P. R. China*
[14] *Indiana University, Bloomington, Indiana 47405, USA*
[15] *Joint Institute for Nuclear Research, 141980 Dubna, Russia*
[16] *KVI/University of Groningen, 9747 AA Groningen, The Netherlands*
[17] *Laboratori Nazionali di Frascati - INFN, 00044 Frascati, Italy*
[18] *Liaoning University, Shenyang 110036, P. R. China*
[19] *Nanjing Normal University, Nanjing 210046, P. R. China*
[20] *Nanjing University, Nanjing 210093, P. R. China*
[21] *Nankai University, Tianjin 300071, P. R. China*
[22] *Peking University, Beijing 100871, P. R. China*
[23] *Seoul National University, Seoul, 151-747 Korea*
[24] *Shandong University, Jinan 250100, P. R. China*
[25] *Shanxi University, Taiyuan 030006, P. R. China*

[26] *Sichuan University, Chengdu 610064, P. R. China*
[27] *Sun Yat-Sen University, Guangzhou 510275, P. R. China*
[28] *The Chinese University of Hong Kong, Shatin, N.T., Hong Kong.*
[29] *The University of Hong Kong, Pokfulam, Hong Kong*
[30] *The University of Tokyo, Tokyo 113-0033 Japan*
[31] *Tsinghua University, Beijing 100084, P. R. China*
[32] *Universitaet Giessen, 35392 Giessen, Germany*
[33] *University of Hawaii, Honolulu, Hawaii 96822, USA*
[34] *University of Minnesota, Minneapolis, MN 55455, USA*
[35] *University of Science and Technology of China, Hefei 230026, P. R. China*
[36] *University of the Punjab, Lahore-54590, Pakistan*
[37] *University of Turin and INFN, Turin, Italy*
[38] *University of Washington, Seattle, WA 98195, USA*
[39] *Wuhan University, Wuhan 430072, P. R. China*
[40] *Zhejiang University, Hangzhou 310027, P. R. China*
[41] *Zhengzhou University, Zhengzhou 450001, P. R. China*

[a] *also at the Moscow Institute of Physics and Technology, Moscow, Russia*
[b] *on leave from the Bogolyubov Institute for Theoretical Physics, Kiev, Ukraine*
[c] *also at the PNPI, Gatchina, Russia*

The decays $\psi' \to \gamma\pi^0$, $\gamma\eta$ and $\gamma\eta'$ are studied using data collected with the BESIII detector at the BEPCII e^+e^- collider. Processes $\psi' \to \gamma\pi^0$ and $\psi' \to \gamma\eta$ are observed for the first time with signal significances of 4.6σ and 4.3σ, respectively. The branching fractions are determined to be: $\mathcal{B}(\psi' \to \gamma\pi^0) = (1.58 \pm 0.40 \pm 0.13) \times 10^{-6}$, $\mathcal{B}(\psi' \to \gamma\eta) = (1.38 \pm 0.48 \pm 0.09) \times 10^{-6}$, and $\mathcal{B}(\psi' \to \gamma\eta') = (126 \pm 3 \pm 8) \times 10^{-6}$, where the first errors are statistical and the second ones systematic.

PACS numbers: 14.40.Gx, 12.38.Qk, 13.25.Gv

The study of vector charmonium radiative decay to a neutral pseudoscalar meson $P = (\pi^0, \eta, \eta')$ provides important tests for various phenomenological mechanisms, such as the vector meson dominance model (VDM) [1–3], two-gluon couplings to $q\bar{q}$ states [2], mixing of $\eta_c - \eta^{(\prime)}$ [4, 5], and final-state radiation by light quarks [1]. Direct contributions from the continuum through a virtual photon: $e^+e^- \to \gamma^* \to \gamma P$ are relevant to the decays of J/ψ, ψ' and ψ'' to γP as discussed recently in Ref. [6]. Furthermore, the possible interference between the charmonium decays and continuum process may play a key role in understanding the difference between J/ψ and ψ' decays into γP [7].

For $P = \eta$ and η', the ratio $R_{J/\psi} \equiv \mathcal{B}(J/\psi \to \gamma\eta)/\mathcal{B}(J/\psi \to \gamma\eta')$ can be predicted by first order perturbation theory [1]. The analogous ratio ($R_{\psi'}$) can be defined for ψ' radiative decays into η and η', and $R_{\psi'} \approx R_{J/\psi}$ is expected [8]. Recently, the CLEO Collaboration reported measurements for the decays of J/ψ, ψ' and ψ'' to γP [8], and no evidence for $\psi' \to \gamma\eta$ or $\gamma\pi^0$ was found. Therefore they obtain $R_{\psi'} \ll R_{J/\psi}$ with $R_{\psi'} < 1.8\%$ at the 90% C.L. and $R_{J/\psi} = (21.1 \pm 0.9)\%$ [8]. Such a small $R_{\psi'}$ is unanticipated, and it poses a significant challenge to our understanding of the $c\bar{c}$ bound states.

The decay $\psi' \to \gamma\pi^0$ is suppressed in QED because the photon can only be produced from final state radiation off one of the quarks. It has also been described via the strong process $\psi' \to ggg \to \rho^*\pi^0$, $\rho^* \to \gamma$ in the VDM [3]. In Ref. [6], the contribution from $\psi' \to \gamma^* \to \gamma\pi^0$ is calculated, and $\mathcal{B}(\psi' \to \gamma\pi^0) \approx 2.19 \times 10^{-7}$ is obtained, which is compatible to the VDM contribution and does not contradict the upper limit of 5.0×10^{-6} (at the 90% C.L.) reported by the CLEO Collaboration [8]. The $\gamma^* - \gamma - \pi^0$ vertex was shown [9] to be characterized by a form factor $F(Q^2)$, where $Q^2 \equiv -q^2$ and q is the four-momentum of the virtual photon γ^*. By using $e^+e^- \to e^+e^-\pi^0$, the form factor was measured in the CLEO [10] and *BABAR* [11] experiments for spacelike nonasymptonic momentum transfer in the range $|q^2| = 1.6 - 8.0$ GeV^2 and $4 - 40$ GeV^2, respectively. The $e^+e^- \to \psi'/\gamma^* \to \gamma\pi^0$ process will be very useful in testing the form factor for timelike photons $Q^2 = -q^2 < 0$ [6].

In this Letter, $\psi' \to \gamma\pi^0$ is studied using $\pi^0 \to \gamma\gamma$ decay, $\psi' \to \gamma\eta$ is measured using $\eta \to \pi^+\pi^-\pi^0$ and $\eta \to \pi^0\pi^0\pi^0$ with $\pi^0 \to \gamma\gamma$, and $\psi' \to \gamma\eta'$ is studied using $\eta' \to \gamma\pi^+\pi^-$ and $\eta' \to \pi^+\pi^-\eta$ with $\eta \to \gamma\gamma$. The analyses use a data sample of 156.4 pb^{-1} collected at the ψ' peak with the BESIII detector operating at BEPCII [12, 13]. By measuring the production of multihadronic events, the number of ψ' decays is found to be $(1.06 \pm 0.04) \times 10^8$ [14]. An independent data sample of 42.6 pb^{-1} taken at $\sqrt{s} = 3.65$ GeV is utilized to determine the potential background contribution from the continuum.

BEPCII is a double-ring e^+e^- collider designed to provide e^+e^- beams with a peak luminosity of 10^{33} cm^{-2}s^{-1} at a beam current of 0.93 A. The cylindrical core of the BESIII detector consists of a helium-based main drift chamber (MDC), a plastic scintillator time-of-flight system (TOF), and a CsI(Tl) electromagnetic calorimeter (EMC), which are all enclosed in a superconducting solenoidal magnet providing a 1.0 T magnetic field. The

solenoid is supported by an octagonal flux-return yoke with resistive plate counter muon identifier modules interleaved with steel. The acceptance of charged particles and photons is 93% over 4π stereo angle, and the charged-particle momentum and photon energy resolutions at 1 GeV are 0.5% and 2.5%, respectively.

The BESIII detector is modeled with a Monte Carlo (MC) simulation based on GEANT4 [15, 16]. EVTGEN [17] is used to generate $\psi' \to \gamma\pi^0, \gamma\eta$, $\gamma\eta'$ events, where the angular distribution of the radiative photon from ψ' decay is $1+\cos^2\theta$ in the ψ' frame. The decay $\eta \to \pi^+\pi^-\pi^0$ is generated according to the Dalitz distribution measured in [18] and $\eta' \to \gamma\pi^+\pi^-$ is simulated assuming it is mediated by $\rho^0 \to \pi^+\pi^-$, while the decays of $\eta \to \pi^0\pi^0\pi^0$ and $\eta' \to \pi^+\pi^-\eta$ are generated with phase space. ψ' decays are simulated by the MC event generator KKMC [19] with known decays modeled by the EVTGEN according to the branching fractions provided by the Particle Data Group (PDG) [20], and the remaining unknown decay modes generated with LUNDCHARM [17].

Charged tracks in BESIII are reconstructed using MDC hits. To optimize the momentum measurement, we select tracks in the polar angle range $|\cos\theta| < 0.93$ and require that they pass within ± 10 cm from the Interaction Point (IP) in the beam direction and within ± 1 cm of the beam line in the plane perpendicular to the beam. All the charged tracks are assumed to be pions, and particle identification (PID) is not required, except in $\eta' \to \gamma\rho$ where the dE/dx information has been used to suppress QED background, most of which is from $e^+e^- \to e^+e^-\gamma$. Either zero or two tracks with net charge zero are required for the final $\pi^0/\eta/\eta'$ decay products.

Electromagnetic showers are reconstructed by clustering EMC crystal energies. The energy deposited in nearby TOF counters is included to improve the reconstruction efficiency and energy resolution. Showers identified as photon candidates must satisfy fiducial and shower-quality requirements. For the $\psi' \to \gamma\eta$ and $\gamma\eta'$ analyses, the photon candidate showers are reconstructed from both the barrel and endcap of the EMC, and showers from barrel region ($|\cos\theta| < 0.8$) must have a minimum energy of 25 MeV, while those in the endcaps ($0.86 < |\cos\theta| < 0.92$) must have at least 50 MeV. The showers in the angular range between the barrel and endcap are poorly reconstructed and excluded from the analyses. To exclude showers from charged particles, a photon must be separated by at least 10° from any charged track. The EMC cluster timing requirements are used to suppress electronic noise and energy deposits unrelated to the event.

Events with the decay modes shown in Table I are selected. Every particle in the final state must be explicitly found, and their vertex must be consistent with the measured beam spot. The sum of four-momenta of all particles is constrained to the known ψ' mass [20] and initial e^+e^- three-momentum in the lab frame. The vertex and full event four-momentum kinematic fits must satisfy $\chi^2_{\rm Vx} < 100$ and $\chi^2_{\rm 4C} < 40$, respectively. For $\eta \to 3\pi^0$, a looser restriction of $\chi^2_{\rm 4C} < 90$ is applied to increase efficiency. Further selections are based on four-momenta from the kinematic fit. In η/η' channels, photon pairs are used to reconstruct π^0 or η candidates if their invariant mass satisfies $M_{\gamma\gamma} \in$ (120, 150) MeV/c^2 or (515, 565) MeV/c^2, respectively.

TABLE I: For each decay mode, the number of signal events (N_S), the number of scaled continuum background events (N_C) in the signal region, the number of expected background events from ψ' decays (N_R) in the signal region, and the MC efficiency (ε) for signal are given. The error on N_S is only the statistical error, and the signal region is defined to be within $\pm 3\sigma$ from the nominal π^0, η, and η' masses.

Modes ($\psi' \to \gamma X$)	N_S	N_C	N_R	ϵ(%)
$\psi' \to \gamma\pi^0$	37.4 ± 9.5	63.5	1.8	21.4
$\psi' \to \gamma\eta(\pi^+\pi^-\pi^0)$	8.9 ± 3.6	2.2	0.0	21.0
$\psi' \to \gamma\eta(\pi^0\pi^0\pi^0)$	3.8 ± 2.3	0.0	1.2	10.7
$\psi' \to \gamma\eta'[\pi^+\pi^-\eta(\gamma\gamma)]$	586 ± 25	0.0	4.7	27.1
$\psi' \to \gamma\eta'(\pi^+\pi^-\gamma)$	1640 ± 44	179.3	111.7	41.0

For the $\psi' \to \gamma\pi^0$ analysis, the primary background comes from the continuum process $e^+e^- \to \gamma\gamma(\gamma)$, where the two energetic photons are distributed in the forward and backward regions. We require that photon candidate showers lie in the barrel region of the EMC to suppress this background. Since π^0 mesons decay isotropically, the angular distribution of photons from π^0 decays is flat in the π^0 helicity frame. However, continuum background events accumulate near $\cos\theta_{\rm decay} = \pm 1$, where $\theta_{\rm decay}$ is the angle of the decay photon in the π^0 helicity frame [14]. To further suppress continuum background, we require $|\cos\theta_{\rm decay}| < 0.5$. Another potentially serious background comes from $e^+e^- \to \gamma\gamma$, in which one γ converts into an e^+e^- pair in the outer part of the MDC. If the track finding algorithm fails to find the track, the two showers in the EMC are identified as isolated photons without associated charged tracks. To suppress this background, the number of MDC hits, N_{hits}, is counted in the sector between the two radial lines connecting the IP and the two-shower positions in the EMC. To take the EMC spacial resolution into account, the sector is extended by 3.5 degrees on both sides. Because of high beam related background level, the hits in the inner 8 MDC layers are not counted in N_{hits}. Figure 1 (a) shows the N_{hits} distribution. As shown in Fig. 1 (b), background from continuum event γ conversions $e^+e^- \to \gamma\gamma$ accumulates in the low mass region. After requiring $N_{hits} \leq 10$, this background is reduced dramatically, while there is still an accumulation of events at the π^0 mass, as shown in Fig. 1 (c).

After applying the above selection criteria, the mass spectra of $\pi^0, \eta,$ and η' candidates are shown in Fig. 2. An unbinned maximum likelihood (ML) fit is used for each analysis to determine the event yields except for $\psi' \to \gamma\eta(\pi^0\pi^0\pi^0)$. The signal probability density function (PDF) in each mode is obtained from MC simulation. The shape for the continuum background is de-

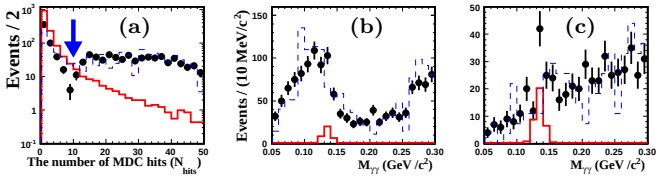

FIG. 1: The distribution of (a) the number of MDC hits, and the two-photon invariant mass distributions for $\gamma\pi^0$ final states (b) without and (c) with the $N_{hits} \leq 10$ requirement. Solid histograms are MC simulated signal for $\psi' \to \gamma\pi^0$; dashed histograms are the luminosity-scaled continuum data, and points are ψ' data. The solid arrow indicates the requirement on N_{hits}.

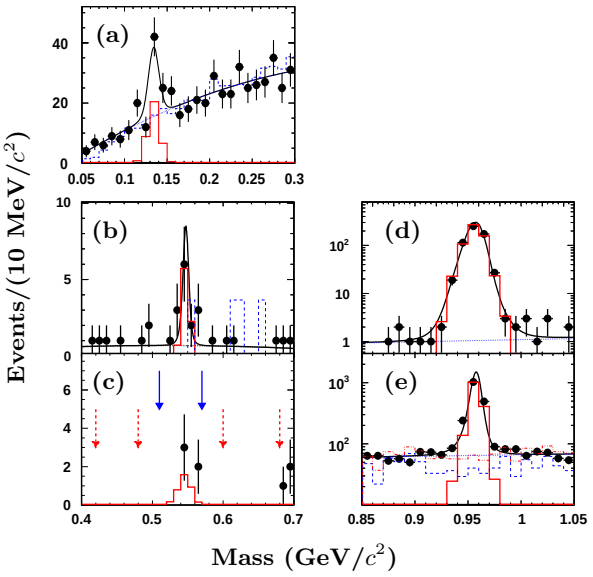

FIG. 2: Mass distributions of the pseudoscalar meson candidates in $\psi' \to \gamma P$: (a) $\gamma\pi^0$, (b) $\gamma\eta(\pi^+\pi^-\pi^0)$; (c) $\gamma\eta(3\pi^0)$; (d) $\gamma\eta'[\pi^+\pi^-\eta(\gamma\gamma)]$; and (e) $\gamma\eta'(\gamma\pi^+\pi^-)$. The crosses are data, the solid histograms are MC simulated signal, and the dashed lines are the continuum backgrounds. Fits are shown as solid lines, background polynomials as dotted lines. In (c), the arrows indicate nominal selection criteria, while the dashed arrows show sidebands. In (e), the dot-dot-dash line shows the sum of the continuum background and the expected background from ψ' decays.

scribed by a second order Chebychev polynomial function, and the yield and its PDF parameters are floated in the fit. The fitting ranges for π^0, η and η' are 0.05–0.30 GeV/c^2, 0.40–0.70 GeV/c^2, and 0.85–1.05 GeV/c^2, respectively. The signal yield for $\psi' \to \gamma\eta(\pi^0\pi^0\pi^0)$ is determined directly by counting the number of events in the signal region, which is in 0.51–0.57 GeV/c^2, about 3 standard deviations from the nominal value of the η mass [20] as shown in Fig. 2 (c), while the sideband regions are defined as 0.42–0.48 GeV/c^2 and 0.60–0.66 GeV/c^2. The signal yields and the efficiencies are summarized in Table I.

The backgrounds remaining after event selection can be divided into two categories. One is from ψ' decays, which can be studied using a sample of 10^8 MC-simulated inclusive ψ' events. The other is from non-resonant processes or initial state radiation to low mass resonances, which can be studied using the continuum data sample collected at a center of mass energy of 3.65 GeV. The expected backgrounds from ψ' decays are listed in Table I, where the number of background events is the number in the signal region, which is defined as within $\pm 3\sigma$ from the nominal π^0, η and η' masses. For $\psi' \to \gamma\pi^0$, the normalized number of events from $\psi' \to \gamma\pi^0\pi^0$ is 1.8 in the π^0 signal range. For $\psi' \to \gamma\eta(\pi^0\pi^0\pi^0)$, there are 1.2 events from the decay of $\psi' \to \gamma\eta(\gamma\gamma)\eta(3\pi^0)$. For $\psi' \to \gamma\eta'(\gamma\pi^+\pi^-)$, the main background from ψ' decays is $\psi' \to \rho^0\pi^0$ which contributes a smooth background. The QED backgrounds for $\psi' \to \gamma\eta'(\pi^+\pi^-\gamma)$ are from $e^+e^- \to \gamma\mu^+\mu^-$ and $e^+e^- \to \gamma e^+e^-$, and both of them give a smooth background under the η' signal peak. For $\psi' \to \gamma\pi^0$, a smooth background is contributed from $e^+e^- \to \gamma\gamma(\gamma)$ events. The cross section for $e^+e^- \to \gamma^* \to \gamma\pi^0(\gamma\eta)$ has been estimated using data collected at $\sqrt{s} = 3.65$ GeV, and the upper limit on the cross section is less than 0.14(0.68) pb at the 90% C.L. Since the continuum cross section is small, we neglect possible interference between $\psi' \to \gamma\pi^0(\eta)$ signal and continuum $\gamma\pi^0(\eta)$. All the backgrounds are summarized in Table I.

The systematic uncertainties for these measurements are summarized in Table II. The uncertainties due to MDC track finding and photon detection are 2% per charged track and 1% per low energy photon. The uncertainty of detecting the high energy photon is less than 0.25% which can be neglected. The systematic errors from π^0 (η) reconstruction is determined to be 1% per π^0 (η) by using a high purity control sample of $J/\psi \to \pi^0\bar{p}p$ ($J/\psi \to \eta\bar{p}p$) decay. The uncertainties due to kinematic fits have been estimated using the control samples with the same event topologies as those in the signal cases, i.e. the same number of charged tracks and same number of photons. The systematic uncertainties due to the dE/dx requirements to identify charged pions in the $\psi' \to \gamma\eta'(\gamma\pi^+\pi^-)$ and N_γ in the $\psi' \to \gamma\pi^0$ are studied by using the control samples of $J/\psi \to \rho\pi$ and $J/\psi \to \gamma\eta(\gamma\gamma)$, respectively, with and without applying these requirements.

In $\psi' \to \gamma\pi^0$, the uncertainty due to the requirement on the MDC hits, $N_{hits} \leq 10$, is studied using a sample of $J/\psi \to \gamma\eta, \eta \to \gamma\gamma$ events. The ratios of events with and without the requirement on the number of MDC hits are obtained for both data and MC simulation. Taking the difference of opening angle between $J/\psi \to \gamma\eta(\gamma\gamma)$ and $\psi' \to \gamma\pi^0$ into account, the difference 3% is considered as the systematic error for the measurement of $\psi' \to \gamma\pi^0$ and is due to the difference in the noise in the MDC for data and MC simulation.

The uncertainty due to the background shape has been estimated by varying the PDF shape and fitting range in the ML fit. For the intermediate decays, the $\eta(\eta')$ branching fractions and uncertainties from the

TABLE II: Summary of systematic errors (%).

Sources	π^0	$\eta\to\pi^+\pi^-\pi^0$	$\eta\to 3\pi^0$	$\eta'\to\pi^+\pi^-\eta(\gamma\gamma)$	$\eta'\to\pi^+\pi^-\gamma$
MDC track finding	–	4	–	4	4
Photon detection	2	2	6	2	1
$\pi^0(\eta)$ reconstruction	–	1	3	1	–
4C kinematic fit	1	3	0	3	2
Background shape	4.8	6.4	–	0	1
Number of ψ'	4	4	4	4	4
Cited branching fractions	0	1.2	0.7	1.7	1.7
MDC hits	3	–	–	–	–
Number of photons	4	–	–	–	–
Total	8.3	9.4	7.8	7.0	6.4

PDG fit [20] are used. The total relative systematic errors on these measurements are 8.3%, 9.4%, 7.8% , 7.0%, and 6.4% for $\psi'\to\gamma\pi^0$, $\psi'\to\gamma\eta(\pi^+\pi^-\pi^0)$, $\psi'\to\gamma\eta(\pi^0\pi^0\pi^0)$, $\psi'\to\gamma\eta'[\pi^+\pi^-\eta(\gamma\gamma)]$, and $\psi'\to\gamma\eta'(\pi^+\pi^-\gamma)$, respectively, as summarized in Table II.

The branching fractions of ψ' decays to γ and a pseudoscalar meson are listed in Table III. Taking the common systematic errors into account, the combined measurements for $\psi'\to\gamma\eta$, $\gamma\eta'$ modes are obtained. The PDG [20] values are also shown in Table III. With considering the background shape uncertainty, we find the signal significance for $\psi'\to\gamma\pi^0(\gamma\eta)$ to be $4.6(4.3)\sigma$, as determined by the ratio of the maximum likelihood value and the likelihood value for a fit where the signal contribution is set to zero.

TABLE III: Branching fractions (10^{-6}) from this analysis, where the first errors are statistical and the second ones are systematic, and the comparison with the PDG values [20].

Mode	BESIII	Combined BESIII	PDG
$\psi'\to\gamma\pi^0$	$1.58\pm0.40\pm0.13$	$1.58\pm0.40\pm0.13$	≤ 5
$\psi'\to\gamma\eta(\pi^+\pi^-\pi^0)$	$1.78\pm0.72\pm0.17$	$1.38\pm0.48\pm0.09$	≤ 2
$\to\gamma\eta(\pi^0\pi^0\pi^0)$	$1.07\pm0.65\pm0.08$		
$\psi'\to\gamma\eta'(\pi^+\pi^-\eta)$	$120\pm5\pm8$	$126\pm3\pm8$	121 ± 8
$\to\gamma\eta'(\pi^+\pi^-\gamma)$	$129\pm3\pm8$		

In summary, we have measured branching fractions for $\psi'\to\gamma\pi^0$, $\psi'\to\gamma\eta$ and $\psi'\to\gamma\eta'$ decays. For the first time, we find evidence for the $\psi'\to\gamma\pi^0$ and $\psi'\to\gamma\eta$ decays with signal significances of 4.6σ and 4.3σ, respectively. The evidence for $\psi'\to\gamma\pi^0$ will yield an experimental constraint on the $\gamma^*\to\gamma\pi^0$ vertex in the timelike regime at $|q^2|=m^2_{\psi'}$ [6]. For the ratio of η and η' production rates from ψ' decays, we obtain $R_{\psi'}=(1.10\pm0.38\pm0.07)\%$, where the statistical and systematic uncertainties from the input branching fractions as listed in Table III have been combined in quadrature after accounting for common systematic errors. This ratio is the first measurement, and it is below the 90% C.L. upper bound determined by the CLEO Collaboration [8]. The corresponding $\eta-\eta'$ production ratio for the J/ψ resonance was measured to be $R_{J/\psi}=(21.1\pm0.9)\%$ [8]. $R_{\psi'}$ is smaller than $R_{J/\psi}$ by an order of magnitude.

The BESIII collaboration thanks the staff of BEPCII and the computing center for their hard efforts. This work is supported in part by the Ministry of Science and Technology of China under Contract No. 2009CB825200; National Natural Science Foundation of China (NSFC) under Contracts Nos. 10625524, 10821063, 10825524, 10835001, 10935007, 10979008; the Chinese Academy of Sciences (CAS) Large-Scale Scientific Facility Program; CAS under Contracts Nos. KJCX2-YW-N29, KJCX2-YW-N45; 100 Talents Program of CAS; Istituto Nazionale di Fisica Nucleare, Italy; Russian Foundation for Basic Research under Contracts Nos. 08-02-92221, 08-02-92200-NSFC-a; Siberian Branch of Russian Academy of Science, joint project No 32 with CAS; U. S. Department of Energy under Contracts Nos. DE-FG02-04ER41291, DE-FG02-91ER40682, DE-FG02-94ER40823; University of Groningen (RuG) and the Helmholtzzentrum fuer Schwerionenforschung GmbH (GSI), Darmstadt; WCU Program of National Research Foundation of Korea under Contract No. R32-2008-000-10155-0.

[1] V. L. Chernyak and A. R. Zhitnitsky, Phys. Rep. **112**, 173 (1984).
[2] J. G. Körner *et al.*, Nucl. Phys. B **229**, 115 (1983).
[3] G. W. Intemann, Phys. Rev. D **27**, 2755 (1983).
[4] H. Fritzsch and J. D. Jackson, Phys. Lett. B **66**, 365 (1977).
[5] K. T. Chao, Nucl. Phys. B **335**, 101 (1990).
[6] J. L. Rosner, Phys. Rev. D **79**, 097301 (2009).
[7] P. Wang *et al.*, Phys. Lett. B **593**, 89 (2004).
[8] T. K. Pedlar *et al.* (CLEO Collaboration), Phys. Rev. D **79**, 111101 (2009).
[9] G. P. Lepage and S. J. Brodsky, Phys. Rev. D **22**,

2157(1980); S. J. Brodsky and G. P. Lepage, Phys. Rev. D **24**, 1808 (1981).
[10] J. Gronberg *et al.* (CLEO Collaboration), Phys. Rev. D **57**, 33 (1998).
[11] B. Aubert *et al.* (*BABAR* Collaboration), Phys. Rev. D **80**, 052002 (2009).
[12] M. Ablikim *et al.* (BES Collaboration), Nucl. Instrum. Methods Phys. Res., Sect. A **614**, 345 (2010).
[13] "Physics at BES-III", edited by K. T. Chao and Y. Wang [Int. J. Mod. Phys. A **24**, Suppl. 1, (2009)]
[14] M. Ablikim *et al.* (BES Collaboration), Phys. Rev. D **81**, 052005 (2010).
[15] S. Agostinelli *et al.* (GEANT4 Collaboration), Nucl. Instrum. Methods Phys. Res. A **506**, 250 (2003).
[16] J. Allison *et al.*, IEEE Trans. Nucl. Sci. **53**, 270 (2006).
[17] R. G. Ping, Chinese Phys. C **32**, 599 (2008).
[18] J. G. Layter *et al.*, Phys. Rev. D **7**, 2565 (1973).
[19] S. Jadach, B. F. L. Ward, and Z. Was, Comput. Phys. Commun. **130**, 260 (2000); Phys. Rev. D **63**, 113009 (2001).
[20] K. Nakamura *et al.* (Particle Data Group), J. Phys. G **37**, 075021 (2010).